A Computer-Aided Hybrid Framework for Early Diagnosis of Breast Cancer

Sourav Pramanik, Debapriya Banik, Debotosh Bhattacharjee and Mita Nasipuri

Abstract We have presented here a novel framework for the early diagnosis of breast cancer. The framework is comprised of two major phases. Firstly, the potential suspicious regions are automatically segmented from the breast thermograms. In the second phase, the segmented suspicious regions are diagnostically classified into benign and malignant cases. For the automatic segmentation of the suspicious regions, a new region-based level-set method named GRL-LSM has been proposed. Initially, the potential suspicious regions are estimated by the proposed adaptive thresholding method (ATM), named GRL. Then, a region-based level set method (LSM) is employed to precisely segment the potentially suspicious regions. As initialization plays a vital role in a region-based LSM, so we have proposed a new automatic initialization technique based on the outcome of our adaptive thresholding method. Moreover, a stopping criterion is proposed to stop the LSM. After the segmentation phase, some higher-order statistical and GLCM-based texture features are extracted and fed into a three-layered feed-forward artificial neural network for classifying the breast thermograms. Fifty breast thermograms with confirmed hot spots are randomly chosen from the DMR-IR database for the experimental purpose. Experimental evaluation shows that our proposed framework can differentiate between malignant and benign breasts with an accuracy of 89.4%, the sensitivity of 86%, and specificity of 90%. Additionally, our segmentation results are validated quantitatively and qualitatively with the respective breast thermograms which were manually delineated by two experts and also with some classical segmentation methods.

S. Pramanik (✉) · D. Banik · D. Bhattacharjee · M. Nasipuri
Department of Computer Science and Engineering, Jadavpur University, Kolkata 700032, India
e-mail: srv.pramanik03327@gmail.com

D. Banik
e-mail: debu.cse88@gmail.com

D. Bhattacharjee
e-mail: debotosh@cse.jdvu.ac.in

M. Nasipuri
e-mail: mnasipuri@cse.jdvu.ac.in

R. Chaki et al. (eds.), *Advanced Computing and Systems for Security*,
Advances in Intelligent Systems and Computing 883,
https://doi.org/10.1007/978-981-13-3702-4_7

Keywords Suspicious region segmentation · GRL-LSM · Feature extraction FANN · Malignant and benign breast thermogram

1 Introduction

Globally, breast cancer is the most commonly diagnosed cancer in women after lung cancer. More than a million of women worldwide are identified with breast cancer every year, which accounts more than 25% of all cases of female cancer [1]. Due to this exponential growth, there is a huge demand for the development of new technologies for the prevention of breast cancer in its early stages. Medical infrared breast thermography has emerged as a promising tool in early diagnosis of breast cancer patients [2]. For the last few decades, there were different researchers in the domain of analysis of breast thermograms to differentiate between normal and abnormal breasts. However, it is very rare to find any allied research to differentiate between malignant and benign breasts. To analyze the acquired breast thermograms, it is very crucial to segment the breast region from the whole image [3]. Due to the vague nature of breast thermograms; most research groups prefer manual or semi-automatic segmentation rather than automatic segmentation [4]. However, the automatic segmentation technique is very much important for the computer-aided analysis of the breast thermograms.

Sathish et al. [4] presented a new segmentation method based on canny edge detection technique to segment the left and the right breast thermogram. Then, for analysis, some features were extracted and fed to a classifier to differentiate between the normal and the abnormal breast thermograms. Prabha et al. [5] made an attempt for the segmentation of the breast thermograms by the reaction-diffusion-based level-set method. After segmentation, authors have extracted some structural-based texture features to perform asymmetry analysis. Mejia et al. [6] proposed a segmentation technique by thresholding and morphological operations. Furthermore, they have also extracted some basic textural features and differentiated the normal breast thermograms from the abnormal ones.

Apart from the breast region segmentation techniques as discussed above, some studies have shown that the suspicious regions (hot regions) captured by an infrared (IR) camera can be a much more significant indicator to justify the level of abnormalities in the breast [7]. Computer-assisted analysis of the suspicious regions after delineating it from the whole breast area defines the degree of malignancy and the level of expansion of the tumor [8]. However, segmentation of the suspicious regions from the thermal breast image is a very challenging task. Because they vary in size and suffer from intensity variation. Moreover, poor edge definition and the chaotic structure of the area of the suspicious region make it difficult to segment. In light of such challenges, considerable progress has been made to segment the suspicious regions, but the results have not been reliable so far. Etehad Tavakol et al. [9] have used k-

means and fuzzy c-means for suspicious regions segmentation. In [10], authors have reported a technique for suspicious region segmentation using minimum variance quantization method followed by morphological operations. However, they did not mention the number of iteration, quantization levels, and radius of the structuring element. In [11], authors have compared three different methods, such as k-means, fuzzy c-means, and level set for the segmentation of suspicious regions and have shown that the level-set method works considerably well in comparison with the other methods. However, in this work, authors have not mentioned how they have initialized the contour points for the LSM. In [12], authors have converted the color breast thermal images to CIELUV color space, then fuzzy c-means clustering technique is used to segment different color regions. Although abnormality cases were classified the major drawback was that malignant cases could not be differentiable from benign cases by their method.

As conferred above, it is very rare to find any research related to the analysis of breast thermograms to differentiate between malignant and benign cases. So, in this study, we have proposed a framework to differentiate between malignant and benign breast thermograms. The framework basically includes two major phases. In the first phase, the potentially suspicious regions are automatically segmented from the breast thermograms. To accomplish this task, a new method GRL-LSM has been proposed. The proposed method comprises of two steps. Initially, the estimation of the potentially suspicious regions is performed by an adaptive thresholding method (ATM) based on global and local image information (GRL). Then, a region-based LSM [13] is employed to accurately segment the potentially suspicious regions. As breast thermograms often suffer from intensity-inhomogeneity and complex background, initialization of a region-based LSM based on global region information often fails to give satisfiable results. Hence, we have proposed a new automatic initialization technique based on the outcome of our initial adaptive thresholding method. In the second phase of our framework, the segmented breast thermograms are analyzed and classified as benign or malignant. To do so, some higher-order statistical features and GLCM-based texture features are extracted from the segmented left and right breasts and fed into a three-layered feed-forward artificial neural network (FANN) with gradient descent training rule. The experiments were carried out on DMR-IR database by randomly choosing 50 breast thermograms (33 benign and 17 malignant) with confirmed hot spots. Our experimental evaluation confirms that our proposed framework can differentiate between the malignant and benign breast more precisely. Additionally, we have validated our segmentation results both quantitatively and qualitatively with the respective breast thermograms which were manually delineated by two medical experts and also with the two classical segmentation methods [9]. It can be observed that our results hold good agreement with the ground truths irrespective of the irregular shape/weak edges of the suspicious regions.

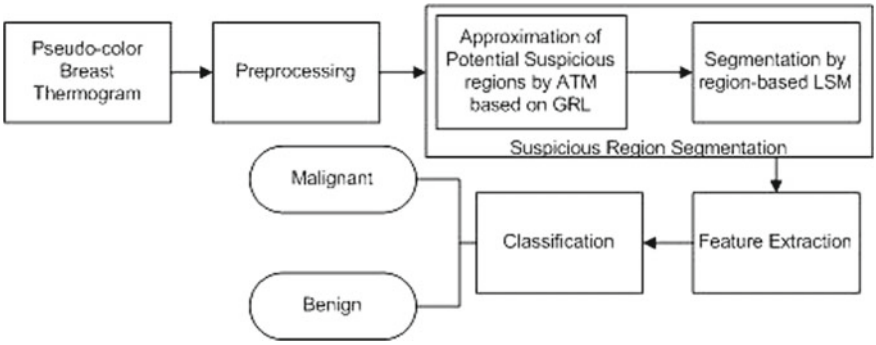

Fig. 1 Flow diagram of the proposed framework

The rest of the paper is arranged as follows. Section 2 demonstrates the proposed system in detail. Section 3 describes the details of an experiment conducted to justify the performance of the proposed framework, and the conclusion is drawn in Sect. 4.

2 Proposed System

Figure 1 shows the flow diagram of the proposed breast abnormality prediction system. Each of the steps will be described in the following subsections.

2.1 Preprocessing

Usually, in the original pseudo-color breast thermogram, colorscale also appears alongside the image, as shown in Fig. 2a, which may mislead the suspicious regions segmentation process. Thus, at the very first step, we manually remove the colorscale from the original breast thermal image, as shown in Fig. 2b. Then, the color breast thermal image is transformed into blue-channel color space as shown in Fig. 2c. From Fig. 2c, it can be seen that the transformation process preserves the location and shape of the thermal features and objects as it is a point-wise transformation. Moreover, most importantly, it has been experimentally seen that the blue-channel image in comparison with the other channels increases the contrast of the high-temperature regions and decreases the contrast of the low-temperature regions.

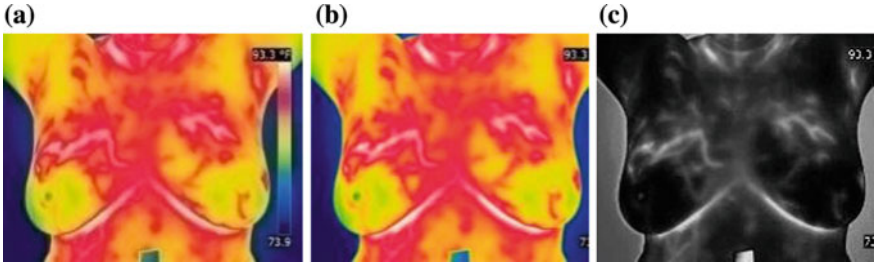

Fig. 2 **a** Original pseudo-color breast thermogram, **b** colorscale-removed image, and **c** corresponding blue-channel image

2.2 Suspicious Regions Segmentation

2.2.1 Approximation of Potentially Suspicious Regions

This method is basically accomplished in two steps: It starts with an approximation of the suspicious regions (hot regions) by an ATM and followed by isolation of the potentially suspicious regions analogous to the suspicious regions. For the approximation of the hot regions, we have proposed here a new ATM based on global-image information regularized by local-image information (GRL). Let us assume that $I^{(b)} : \omega \rightarrow \mathcal{R}^{+}$ be the blue-channel thermal breast image, where $\omega \subset \mathcal{R}^{2}$ is the image domain. In this proposed method, a threshold value is adaptively calculated for each pixel in the blue-channel image $I^{(b)}$ to identify it as a suspicious region pixel or a normal region pixel. Usually, the intensities in the center area of a suspicious region have superiority over the entire image and which gradually decreases toward the boundary. Thus, the pixel belonging to the center area of the suspicious region can be easily classified as a suspicious region pixel using a global threshold value. However, the global threshold will not work when the pixel in the suspicious region has a very small difference in intensity with the normal tissue pixel. In this case, the classification of such pixel completely depends on its neighboring pixels. Thus, we have used a combination of the global superiority and the local dependency of a pixel in the image to compute a threshold for it. The threshold value T(x, y) for the pixel $p_c \in I^{(b)}$ is computed by Eq. (1).

$$T(x, y) = I^{(b)}_{avg} + \delta * \left(I^{(b)}_{max} - I^{(b)}_{min}\right) \tag{1}$$

$$\delta = \frac{1}{|w|} \sum\nolimits_{p_i \in w(p_c)} s(p_c == p_i) \tag{2}$$

$$s(\cdot) = \begin{cases} 1, \text{ if } p_c == p_i \\ 0, \text{ otherwise} \end{cases} \tag{3}$$

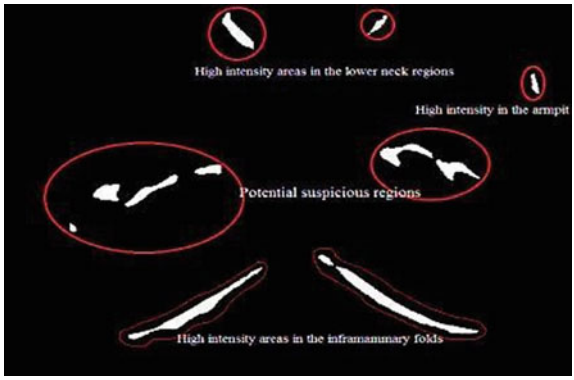

Fig. 3 Different probably high-intensity zones in a breast thermogram

where, $I^{(b)}_{avg}$ is an average intensity of the image $I^{(b)}$, $I^{(b)}_{max}$ and $I^{(b)}_{min}$ are the maximum and minimum intensity of the image $I^{(b)}$, δ is a thresholding control parameter, $|w|$ is the size of the square window around the centered pixel p_c, and (x, y) is the coordinate of the pixel p_c. In our case, a 3×3 window size is considered. Now, if a pixel $p_c(x, y) \in I^{(b)} \geq T(x, y)$, it is classified as the suspicious region pixel; otherwise, it is classified as a normal tissue region pixel.

Once the suspicious regions (or hot regions) are approximated, the next goal is to identify the potentially suspicious regions. Let B_{SR} be the binary image containing the hot region areas, as shown in Fig. 3. In Fig. 3, a white region encircled with red colors exhibits the hot region areas and the possible suspicious regions are located approximately at the center part of the image. Therefore, if we calculate the centroids of all the hot regions, the centroids of the possible suspicious regions will be greater than the centroids of the regions located in the lower-neck areas and armpits. Similarly, it is less than the centroid of the inframammary fold regions. Hence, in this paper, potentially suspicious regions are isolated based on the centroid information. Note that the proposed adaptive thresholding method based on GRL approximates the highest intensity zones in the potentially suspicious regions. Therefore, to accurately segment the potentially suspicious regions, GRL results are used to initialize the LSM which we have discussed in the next section.

2.2.2 Segmentation by Region-Based Level-Set Method (LSM)

To precisely segment the potentially suspicious regions from the breast thermograms, we have used the Chan-Vese (CV) level-set method (LSM) [13]. Basically, the CV-LSM is a region-based method where contours are driven on the basis of intensity, color or texture information. The suspicious regions in a breast thermogram are often susceptible to noise, poor edge definition, and have irregular shapes. So to address the aforesaid problems, CV-LSM is employed as this method gives robust results

despite such issues [14]. In the CV-level-set method, the energy functional is defined as follows:

$$E_{CV}(\varphi, c_i) = \beta \int_{\omega} \delta_{\varepsilon}(\varphi(x, y))|\nabla\varphi(x, y)|dxdy + \sum_{i=1}^{2} \alpha_i \int_{\omega} \left|I^B(x, y) - c_i\right|^2 H^i dxdy \quad (4)$$

where $\varphi : \omega \to \mathcal{R}$ is the level-set function which is used to implicitly represent the closed contour $C(q) : \mathcal{R} \to \omega$, c_1 and c_1 are two constants computed inside and outside of C as the average intensity and play a very crucial role for the evolution of the contour C, α_1 and α_2 are two positive-fixed parameters used as trade-off between the first and second terms of the data fitting term in (4), $H^1 = H_{\varepsilon}(\varphi(x, y))$ and $H^2 = (1 - H_{\varepsilon}(\varphi(x, y)))$ are the smooth approximation of the Heaviside function, the first term on the right-hand side of (4) is called the contour length term which is used to smooth the φ and the second term is called data fitting term that is used to drive the φ toward the object boundary, δ_{ε} signifies the Dirac delta function. Typically, in this work, let us assume that the zero-level set φ is negative inside the closed contour C, positive outside of C, and zero on the C, respectively [15].

The initialization of the level-set function plays a crucial role in driving the level set for accurate detection of the suspicious regions. In practice, if the initialization is apart from the original region of interest boundaries, the zero level set will take huge iterations to segment the region of interest. Most of the works used manual initialization, which required thorough domain knowledge and also a very much labor-intensive procedure. Therefore, in this work, the outcome of the ATM is used here to precisely initialize the level-set function (LSF) φ. The LSF is initialized as follows: Let, B represents the binary image containing different potentially suspicious regions as obtained from the previous section.

To initialize the level-set function $\varphi(x, y)$, B should satisfy the property of φ [15], so we have computed Euclidean distance transform (EDT) on the binary image B(x, y) as in Eq. (6)

Let $p(x, y) \in B$ be any pixel in B and $q_n(x, y) \in B$ be non-zero pixels in $\{B|q_n(x, y) = 1\}$

$$B^p_{EDT}(x, y) = \underset{n=1,2,..,L}{\text{Min}} \left\| p - q_n \right\| \quad (6)$$

where L is the number of non-zero pixels in B and ||.|| denotes the Euclidean distance.

For a binary image B(x, y) in Fig. 4, where the zero pixels represent the background and the non-zero pixels enclosed with red color represent a potentially suspicious region. For each pixel in B(x, y) EDT is computed and mapped to $B_{EDT}(x, y)$. Finally, $B_{EDT}(x, y)$ is initialized to the level-set function to drive the level set.

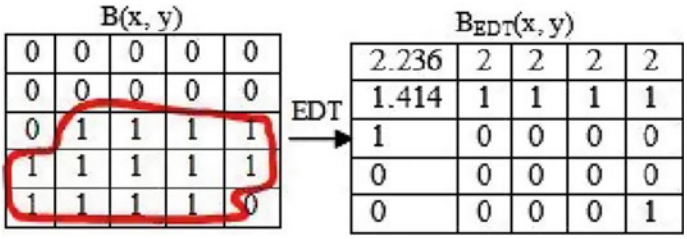

Fig. 4 Euclidean distance transform of B(x, y)

Now, the initial zero-level-set function φ can be defined as follows:

$$\varphi(x, y, t = 0) = \mathrm{B}^{\mathrm{p}}_{\mathrm{EDT}}(x, y) \tag{7}$$

In each iteration, the energy function (4) is minimized with respect to φ and c_i by considering the Euler–Lagrange equations and updating φ using the gradient descent method:

$$\begin{aligned} \frac{\partial \varphi(\mathrm{x}, \mathrm{y})}{\partial \mathrm{t}} &= \delta_{\varepsilon}(\varphi(\mathrm{x}, \mathrm{y}))\left[-\alpha_1 (I^B(x, y) - c_1)^2 + \alpha_2 (I^B(x, y) - c_2)^2 + \beta div\left(\frac{\nabla \varphi}{|\nabla \varphi|}\right)\right] \\ \varphi(x, y, t = 0) &= \mathrm{B}^{\mathrm{p}}_{\mathrm{EDT}}(x, y) \end{aligned} \tag{8}$$

Similarly, c_1 and c_2 are updated as follows:

$$c_i = \frac{\int_{\omega} I^{(b)}(x, y) H^i dx dy}{\int_{\omega} H^i dx dy}$$

Generally, in region-based CV-LSM method, the criteria to stop the curve evolution are set manually by stating the value of N (no. of iterations) or by minimizing the energy term for the level-set function. The drawback of the prior stopping terms in the domain of thermal breast imaging is that the image is prone to intensity variation and weak edges, which may lead to over or under segmentation. So, we have proposed a new technique to stop the curve automatically.

Let, the level-set function for $(N - 1)$th, Nth, and $(N + 1)$th iteration be $\varphi^{N-1}_{(x,y)}$, $\varphi^{N}_{(x,y)}$ and $\varphi^{N+1}_{(x,y)}$. The curve will stop automatically if the correlation coefficient (r) satisfies for N > 1 Eq. (9)

$$r(\varphi^{N-1}_{(x,y)}, \varphi^{N}_{(x,y)}) \approx 1 \approx r(\varphi^{N}_{(x,y)}, \varphi^{N+1}_{(x,y)}) \tag{9}$$

Finally, the resultant curve will segment all the potentially suspicious regions more precisely. Figure 5 represents automatic segmentation result of a breast thermogram by our proposed method.

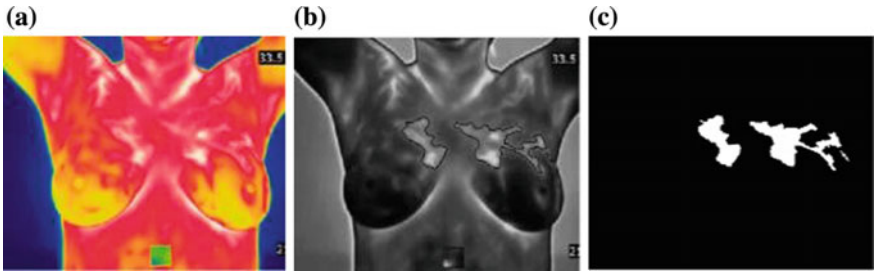

Fig. 5 **a** Initial breast thermogram, **b** segmentation by proposed method, and **c** final-segmented binary image

2.3 Feature Extraction

After the segmentation of the potentially suspicious regions, a set of features is extracted from each of the breast (left and right) of each patient. Here, we have considered two variants of feature sets: GLCM-based texture features and higher-order statistical moments. GLCM of an image is the measure of how often various combinations of gray levels co-occur in an image. From the GLCM, we have computed entropy, contrast, correlation, energy, and homogeneity [4]. It may be noted that texture analysis plays a crucial role in the areas of infrared image analysis since temperature variations in thermogram images are represented by its texture. Apart from the textural features, the statistical moments are also calculated up to order 20. The first-order moment is the mean of the pixels values in the block and is calculated using Eq. (10) [16]. The remaining higher-order normalized moments are calculated by Eq. (11)

$$M^{(1)} = \frac{1}{N}\sum_{i=1}^{N} x_i \tag{10}$$

$$M^{(q)} = \frac{1}{\sigma^2}\sum_{i=1}^{N} \left(x_i - M^{(1)}\right)^q \tag{11}$$

where N is the number of non-zero pixels in the region of interest, $q = 2, 3, \ldots, 20$ and σ is the standard deviation.

After the computation of the five GLCM-based texture features and statistical moments up to order 20, they are concatenated to form a 25-element feature vector for each left and right breast.

Let $\left[f_v^{(L)}\right]_{1\times 25}$ and $\left[f_v^{(R)}\right]_{1\times 25}$ demonstrate the feature vectors of left and right breast thermogram of each patient. The vectors $f_v^{(L)}$ and $f_v^{(R)}$ are defined as

$$f_v^{(L)} = \left[f_1^{L\_GLCM}, f_2^{L\_GLCM}, \ldots, f_5^{L\_GLCM}, f_1^{L\_M}, f_2^{L\_M}, \ldots, f_{20}^{L\_M}\right] \tag{12}$$

$$f_v^{(R)} = \left[f_1^{R\_GLCM}, f_2^{R\_GLCM}, \ldots, f_5^{R\_GLCM}, f_1^{R\_M}, f_2^{R\_M}, \ldots, f_{20}^{R\_M} \right] \tag{13}$$

Finally, the asymmetry features are calculated for each patient's breast thermogram by taking the absolute difference between $f_v^{(L)}$ and $f_v^{(R)}$. Let $[F]_{1\times 25}$ be the asymmetry feature vector of a patient's breast thermogram and is defined as

$$F = \left| f_v^{(L)} - f_v^{(R)} \right| \tag{14}$$

2.4 Classifier Design

A three-layered feed-forward artificial neural network (FANN) [17] is used to classify the breast thermograms into malignant and benign. A total of 25 neurons in the input layer of the network are considered to fit the 25-element feature vector. The linear transformation function is used in the input layer. Here, one hidden layer is considered that consists of 50 neurons and the sigmoid transfer function is used for all the nodes present in both the hidden and output layers. Since our problem of classification is a binary problem, we have considered one neuron in the output layer. For the training of the network, the Levenberg–Marquardt back-propagation algorithm (with learning rate = 0.1) is used. A total of 30 breast thermograms (10 malignant and 20 benign) are randomly chosen from a set of 50 thermal breast images (17 malignant and 33 benign) to train the network. Remaining breast thermograms are used to test the network.

3 Experimental Results and Discussion

3.1 Database Collection

The breast thermograms used in this research work are collected from the existing DMR-IR (Database for Mastology Research) Database [18]. DMR-IR is an open-access online database that consists of breast thermograms of 287 patients. The dataset includes breast thermograms of normal, benign, and malignant patients. From the set of benign and malignant breast thermograms, 50 breast thermograms with confirmed hot spots are randomly selected for our work of which 33 thermograms are of benign breasts and 17 thermograms are of malignant breasts.

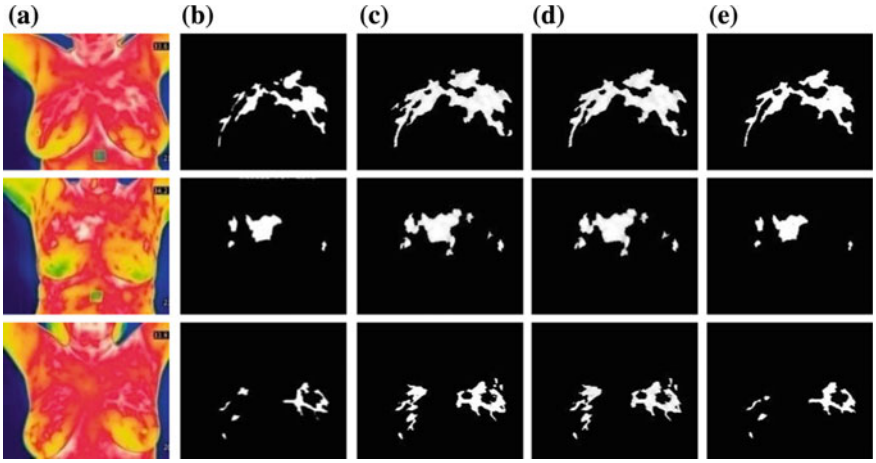

Fig. 6 **a** Breast thermal image, **b** ground truth, **c** segmentation by K-means method, **d** segmentation by Fuzzy c-means method, and **e** our proposed method

3.2 Performance Assessment

In this section, we have evaluated the effectiveness of our proposed segmentation method using qualitative and quantitative performance assessment. To compare the segmentation results, two sets of ground truth images are developed by two different medical experts in this relevant field.

For the purpose of qualitative analysis, our proposed segmentation method is compared visually with the average ground truths and also with some of the traditional segmentation methods, viz k-means and fuzzy c-means as mentioned in [9]. From Fig. 6, it can be effectually envisioned that our proposed method holds good agreement with the ground truth in comparison with the other traditional methods.

Apart from visual analysis, quantitative analysis is also accomplished to measure the accuracy of our segmentation results. Some of the traditional measures commonly used for quantitative analysis are Jaccard Index (JC), Dice Similarity (DS), Tanimoto (TN), and Volume Similarity (VS) [19]. Here we have compared our segmentation method with some of the traditional segmentation approaches as discussed above. The mean for each of the quantitative measures is evaluated for the two sets of ground truth (GT_1 and GT_2), respectively, as shown in Table 1. From Table 1, it can be seen that our proposed method noticeably outperforms when compared with the two classical segmentation methods.

Table 1 Overlap similarity measure for K-means, Fuzzy c-means, and the Proposed method

Method	JC		DS		TN		VS	
	GT_1	GT_2	GT_1	GT_2	GT_1	GT_2	GT_1	GT_2
K-means	0.571	0.572	0.716	0.717	0.925	0.926	0.779	0.776
Fuzzy c-means	0.588	0.589	0.730	0.731	0.931	0.931	0.809	0.805
Proposed method	0.699	0.704	0.820	0.823	0.964	0.965	0.932	0.935

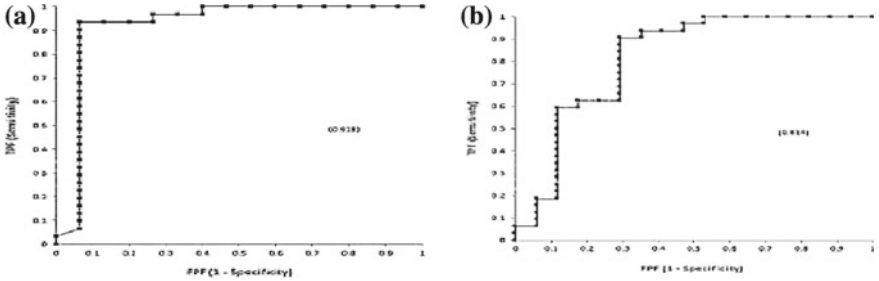

Fig. 7 **a** ROC curve for our method, and **b** ROC curve for a method without segmentation

3.3 Classification

In this section, we have shown the effectiveness of our segmentation results for the differentiation of the malignant and benign thermal breast images. As discussed in Sect. 2, the 25-element feature vector is formed for each patient's breast thermogram, which is then fed to the three-layered feed-forward artificial neural network (FANN) for the classification. Thus, three traditional performance measures such as accuracy, sensitivity, and specificity are calculated based on the classification results [20]. We have also quantified our classification results using receiver operating characteristic (ROC) curve. The area under the curve (AUC) is very much informative for the analysis of the system results, which typically lies between 0.5 and 1 [20]. AUC near to 1 signifies that the discriminating ability of the system is considerably well. In this work, the obtained accuracy, sensitivity, and specificity are 89.4%, 86%, and 90%, respectively. Figure 7a shows the ROC curve for the proposed method. The obtained AUC value is 0.919 and attained 100% true positive recognition at 0.4 false positive rates.

To verify the efficacy of the proposed system (suspicious regions segmentation + feature extraction) over the system without suspicious regions segmentation, the same set of features are extracted from each patient's breast thermogram without segmenting the suspicious regions and used for classification. Table 2 summarizes the performance measures of the classification results. The result confirms that our proposed method outperforms over the compared method.

Table 2 Comparison of classification performance measures

Methods	Accuracy (%)	Sensitivity (%)	Specificity (%)	Area under the ROC curve
Proposed method	89.4	86	90	0.919
Method without segmentation of the suspicious regions	78	50	93	0.814

4 Conclusion

Automatic segmentation of potentially suspicious regions from the breast thermograms plays a crucial role in the computer-assisted analysis of the breast thermograms and differentiating between benign and malignant breasts. Hence, in this paper, we have proposed a framework to automatically segment the potentially suspicious regions and analyzed the segmented regions to differentiate between benign and malignant breasts. Most of the automatic segmentation algorithm claimed till date has some human intervention either to specify the initialization point or to stop the evolution of the curve. However, our system does not require any human intervention and can segment the potentially suspicious regions precisely. The evaluation of experimental results reveals that our proposed framework can effectively differentiate between malignant and benign breasts. Moreover, our segmentation method outperforms in terms of performance measurement when compared to other traditional methods. We believe that our system can serve as a second option to a radiologist for early diagnosis of breast cancer and differentiate between the malignant and benign cases. It is significant to say that the performance of classification would have been much better if some strong feature sets were used in our study. So our future direction would be to improve the classification performance by considering powerful feature sets.

Acknowledgements Authors are thankful to DBT, Govt. of India for funding a project with Grant no. BT/533/NE/TBP/2014. Sourav Pramanik is also thankful to Ministry of Electronics and Information Technology (MeitY), Govt. of India, for providing him Ph.D.Fellowship under Visvesvaraya Ph.D. scheme.

References

1. http://www.wcrf.org/int/cancer-facts-figures/data-specific-cancers/breast-cancer-statistics. Accessed 5 Aug 2017
2. Jones, B.F.: A reappraisal of the use of infrared thermal image analysis in medicine. IEEE Trans. Med. Imaging **ED-17**, 1019–1027 (1998)
3. Francis, S.V., Sasikala, M., Saranya, S.: Detection of breast abnormality from thermo grams using curvelet transform based feature extraction. J. Med. Syst. **38**(4), 1–9 (2014)

4. Sathish, D., Kamath, S., Prasad, K., Kadavigere, R., Martis, R.J.: Asymmetry analysis of breast thermograms using automated segmentation and texture features. J. Signal Image Video Process. **10**, 1–8 (2016)
5. Prabha, S., Anandh, K.R., Sujatha, C.M., Ramakrishnan, S.: Total variation based edge enhancement for level set segmentation and asymmetry analysis in breast thermograms. In: IEEE International Conference on Engineering in Medicine and Biology Society (EMBC) (2014)
6. Mejia, T.M., Perez, M.G., Andaluz, V.H., Concil, A.: Automatic segmentation and analysis of thermograms using texture descriptors for breast cancer detection. In: IEEE International Asia-Pacific Conference on Computer Aided System Engineering (2015)
7. Etehad Tavakol, M., Ng, E.Y.K.: Breast thermography as a potential non-contact method in the early detection of cancer: a review. J. Mech. Med. Biol. **13**(2), 1–20 (2013)
8. Qi, H., Kuruganti, P.T., Snyder, W.E.: Detecting breast cancer from thermal infrared images by asymmetry analysis. In: Biomedical Engineering Handbook, pp. 27.1–27.14. CRC, Boca Raton (2016)
9. Etehad Tavakol, M., Sadri, S., Ng, E.Y.K.: Application of K- and fuzzy c-means for color segmentation of thermal infrared breast images. J. Med. Syst. **34**, 35–42 (2010)
10. Milosevic, M., Jankovic, D., Peulic, A.: Thermography based breast cancer detection using texture features and minimum variance quantization. EXCLI J. **13**, 1204–1215 (2014)
11. Golestani, N., Etehad Tavakol, M., Ng, E.Y.K.: Level set method for segmentation of infrared breast thermograms. EXCLI J. **13**, 241–251 (2014)
12. Pramanik, S., Bhowmik, M.K., Bhattacharjee, D., Nasipuri, M.: Segmentation and analysis of breast thermograms for abnormality prediction using hybrid intelligent techniques. In: Hybrid Soft Computing for Image Segmentation, pp. 255–289. Springer (2016)
13. Chan, T., Vese, L.: Active contours without edges. IEEE Trans. Image Proc. **10**, 266–277 (2001)
14. Osher, S., Fedkiw, R.: Level set methods and dynamic implicit surfaces. Appl. Math. Sci. **153**, 1–82, 119–124 (2002)
15. Cheng, L., Yang, J., Fan, X., Zhu, Y.: A generalized level set formulation of the Mumford-Shah functional for brain MR image segmentation. In: IPMI 2005. LNCS 3565, pp. 418-430 (2005)
16. Gupta, A.: Groundwork of Mathematical Probability and Statistics, 3rd edn. Academic Publishers, Calcutta, India (1995)
17. Pramanik, S., Bhattacharjee, D., Nasipuri, M.: Texture analysis of breast thermogram for differentiation of malignant and benign breast. In: IEEE International Conference on Advances in Computing, Communications, and Informatics (2016)
18. Silva, L.F., Saade, D.C.M., Sequeiros-Olivera, G.O., Silva, A.C., Paiva, A. C., Bravo, R.S., Conci, A.: A new database for breast research with infrared image. J. Med. Imaging Health Inform. **4**(1), 92–100(9) (2014)
19. Cardenes, Ruben, de Luis-Garcia, Rodrigo, Bach-Cuadra, Meritxell: A multidimensional segmentation evaluation for medical image data. J. Comput. Methods Programs Biomed. **96**(2), 108–124 (2009)
20. Acharya, U.R., Ng, E.Y.K., Tan, J.H., Sree, S.V.: Thermography based breast cancer detection using texture features and support vector machine. J. Med. Syst. **36**(3), 1503–1510 (2012)